

# An Improved Current-Limiting Strategy for Shunt Active Power Filter (SAPF) Using Particle Swarm Optimization (PSO)

Wu Cao, Mumu Wu and Jianfeng Zhao

Department of Electrical Engineering  
Southeast University, Nanjing, Jiangsu, 210096, China  
Email: caowu\_ee@seu.edu.cn, [wumumu\\_seu@163.com](mailto:wumumu_seu@163.com),  
[jianfeng\\_zhao@seu.edu.cn](mailto:jianfeng_zhao@seu.edu.cn)

Weiqun Liu and Yu Lu

NARI-Relays Electric Co. Ltd  
Nanjing, Jiangsu, 211100, China  
Email: [shaozx@nrec.com](mailto:shaozx@nrec.com), [liuweiqun@nrec.com](mailto:liuweiqun@nrec.com)

**Abstract**—The current-limiting strategy for shunt active power filter (SAPF) will be activated automatically, when the compensation-capacity need exceeds the rated capacity. However, the traditional current-limiting strategy cannot realize the comprehensive protection with optimum objectives. The paper firstly reveals the essential of the current-limiting demands for the comprehensive protection of SAPF, namely the limiting control objects: 1) the root mean square (RMS) of the compensation current (mainly for the overheat protection of the IGBT and inductor); 2) the instantaneous wave of compensation current (mainly for the accurate current control and IGBT I<sub>nom</sub> specification) and 3) the instantaneous wave of PWM-VSC modulation voltage (for the need of liner close-loop control). Secondly, the paper proposes an improved current-limiting scheme based on particle swarm optimization (PSO) to achieve the two optimization targets: 1) the minimization THD for the grid-side current; 2) the maximization utilization ratio for the capacity of the SAPF. The main advantage lies on the optimum limiting ratios of each harmonic order are calculated in real time respectively to achieve the flexible and liner limiting control. Finally, simulation and experiment verify the effectiveness of the proposed strategy.

**Keywords**—Shunt active power filter; Current-limiting demands; Current-limiting strategy; Particle swarm optimization

## I. INTRODUCTION

Shunt active power filter (SAPF) has gradually become a preferred method to suppress harmonics for its real time compensation, fast dynamic response and no resonance with power grid [1]-[4]. However, when the nonlinear loads increase suddenly, or some types of short-circuit or open-circuit fault occur, the strong impact currents resulting from these faults will be included in the reference currents, which will lead to the over-current fault and over-modulation fault of SAPF [5]-[8]. In the practical engineering application, the simplest way to solve the above faults is blocking the pulses. Although this method is fast and reliable [9]-[11], the SAPF will quit operation and sometimes the small-capacity SAPF will be unable to operate all the time on account of the excessive compensation requirement. Therefore, two typical current-limiting control strategies are proposed to overcome

This work was supported by the National Science Foundation of China under Grant 51607037, and the Innovation foundation for Combination of Industry and Scientific Research of Jiangsu Province Grant BY2016076-09.

this issue as follows: the truncated control and the equal-proportion control. However, the former introduces extra undesired harmonic currents into power system, while the latter has a low utilization rate of SAPF [12]-[15]. To increase the utilization rate of SAPF or reduce the THD of grid-side current, the traditional current-limiting control strategies are improved with the optimum limiting ratios of each harmonic calculated by PSO in this paper. Finally, the effectiveness of the proposed strategy is verified by simulation and experiment.

## II. ANALYSIS ON CURRENT-LIMITING DEMANDS

### A. Current-limiting demand according to dc-link voltage utilization

The topology structure of main circuit for Shunt active power filter (SAPF) is shown in Fig.1.

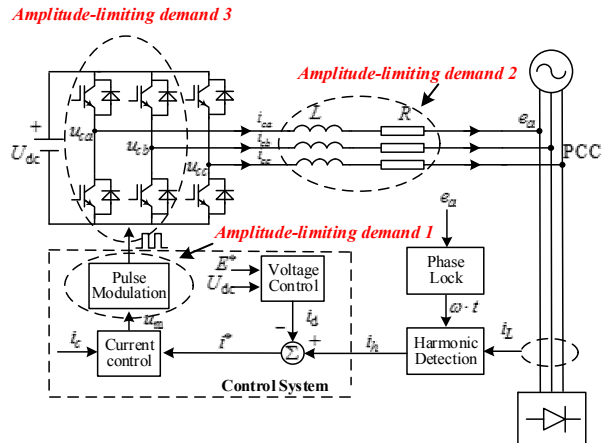


Figure. 1. System mechanism diagram of SAPF.

In Fig.1,  $U_{dc}$  is the dc-link voltage,  $R$  and  $L$  are the equivalent resistance and filter inductance,  $i_{cx}$ ,  $u_{cx}$  and  $e_x$  are APF output currents, APF output voltages and grid-side voltage, respectively, where  $x=a, b$  and  $c$ .

According to Fig.1, taking A phase as an example, the mathematical model can be described by following expression:

$$L \frac{di_{ca}}{dt} + Ri_{ca} = U_{ca} - e_a \quad (1)$$

$$e_a = E_m \cos(\omega t) \quad (2)$$

Where,  $E_m$  and  $\omega$  represent the RMS value and angular frequency of  $e_a$ , respectively.

The output current of the SAPF can be divided into three parts: the fundamental active current component  $i_{cap}$ , reactive component  $i_{caq}$  and harmonic component  $i_{can}$ . The entire output current can be described by the following expression:

$$i_{ca} = I_{cap} \cos(\omega t) + I_{caq} \cos(\omega t + \theta_1) + \sum_{n=6k \pm 1} I_{can} \cos(n\omega t + \theta_n) \quad (3)$$

Where,  $\theta_1$  and  $\theta_n$  represent initial phase of reactive component  $i_{caq}$  and harmonic component  $i_{can}$ , respectively.

Referring to (1), (2) and (3), and neglect  $R$ , the reference voltage of SAPF can be obtained:

$$U_{refa} = E_m \cos(\omega t) + \omega LI_{cap} \cos(\omega t) + \omega LI_{caq} \cos(\omega t + \theta_1) + \sum_{n=6k \pm 1} n\omega LI_{can} \cos(n\omega t + \theta_n) \quad (4)$$

When modulation index  $M = 1$ , the maximum output voltage will be  $U_{dc} / 2$ , therefore the maximum value of the reference voltage require no more than  $U_{dc} / 2$  to have better compensation effect, which can be described by the following expression:

$$\frac{U_{dc}}{2} \geq \left| E_m \cos(\alpha) + \omega LI_{cap} \cos(\alpha) + \omega LI_{caq} \cos(\alpha + \theta_1) + \sum_{n=6k \pm 1} n\omega LI_{can} \cos(n\alpha + \theta_n) \right|_{max} \quad (5)$$

Above analysis shows that when the nonlinear loads increase, or some types of short-circuit or open-circuit fault occur near the PCC, the strong impact current will inevitably result in  $U_{refa} > U_{dc} / 2$ , which means over-modulation occur. In this case, the current-limiting process in a shunt APF is necessary.

### B. Current-limiting demand according to the root mean square (RMS) of the compensation current

Current-limiting demand according to the root mean square of the compensation current mainly occurs in IGBT and grid-connected inductance. For the former, generally, a limited policy will be adopted. For the latter, the over-current fault will cause the over temperature which affect the output characteristic curve of the reactor inevitably, in this case, the temperature switch is adopted instead of a limited policy to guarantee the performance of SAPF, generally, the SAPF shuts down immediately when the temperature of grid-connected inductance exceeds the threshold.

The maximum junction temperature  $T_{jmax}$  is required to less than  $150^\circ\text{C}$  in order to prevent IGBT from the damage of thermal breakdown. Literature [16] provides the formula for calculating the junction temperature  $T_j$  according to heat consumption and model. The relationship between the junction temperature and the effective value of the compensating current IRMS can be studied by the IGBT power loss simulation software. On this basis, the mathematical relationship is described by the following expression:

$$T_j = T_f + kI_{RMS} \quad (6)$$

The relationship between  $T_j$  and  $I_{RMS}$  is approximately linear according to the above formula. In formula (6),  $T_f$  represent the surface temperature of the heat sink,  $k$  is the temperature coefficient, which is related to the power loss of IGBT, the loss of reverse restore diode, junction-to-case thermal resistance, and the heat resistance of the IGBT shell and the radiator.

Amplitude-limiting demand according to the root mean square of the compensation current can be described by (7) on the basis of above analysis.

$$\sqrt{I_{cap\_rms}^2 + I_{caq\_rms}^2 + \sum_{n=2k \pm 1} I_{can\_rms}^2} \leq \frac{T_{jmax} - T_f}{k} \quad (7)$$

### C. Current-limiting demand according to the instantaneous wave of compensation current

Current-limiting demand according to the instantaneous wave of compensation current mainly occurs in IGBT and grid-connected inductance. For the former, the peak of harmonic current need to meet (8) to prevent IGBT from breaking down by blocking the pulses.

$$I_{p\_max} \geq \left| I_{cap} \cos(\alpha) + I_{caq} \cos(\alpha + \theta_1) + \sum_{n=6k \pm 1} I_{can} \cos(n\alpha + \theta_n) \right|_{max} \quad (8)$$

Where  $I_{can}$  is the peak value of each harmonic current,  $I_{prms}$  and  $I_{qrms}$  represent the peak value of active current component and reactive current component, respectively. In addition,  $I_{p\_max}$  is decided by the rated peak-value withstand current of IGBT which is generally set to  $2I_{RMS}$ .

For the latter, the peak value of each harmonic current need to meet certain constraints respectively according to the following deduction so that the output current can change quicker than the current reference to realize precisely track.

Taking A phase as an example, the mathematical model of SAPF can be described as (1), ignore  $R$  in a switching cycle:

$$L \frac{\Delta i}{T_1} = U_{ca} - e_a \quad (9)$$

Where  $T_1$  represents the conduction time during a switching cycle. In a cycle of the reference current, the maximum change rate of current occur at the zero crossing point, referring to (9), amplitude-limiting demand according to current peak value can be given:

$$\frac{I_{can} \sin(n\omega T_1)}{T_1} \Big|_{n\omega T_1 \rightarrow 0} = I_{can} \cdot n\omega \leq \frac{\Delta i}{T_1} = \frac{U_{ca} - e_a}{L} \quad (10)$$

Where  $U_{ca}$  is the dc-link voltage,  $n$  represent harmonic order. In addition,  $e_a$  represent the grid side voltage at zero-crossing point of each harmonic current which is generally set to 311V.

### III. IMPROVED CURRENT-LIMITING CONTROL METHOD USING PARTICLE SWARM OPTIMIZATION

#### A. Optimal current-limiting strategy

Taking three-phase three-wire system as an example, in the premise of satisfying the restrictions of (5), (7), (8) and (10), the utilization rate of shunt APF should be optimal. Considering that particle swarm optimization (PSO) is proposed in this paper to solve the nonlinear multivariate optimum problem with constraints.

PSO was originally proposed by Kennedy and Eberhart. It is a kind of evolution-based heuristic inspired by the foraging behaviors of flock of birds. The concept of "group" and "evolution" are included in particle swarm algorithm, and operates according to the fitness. PSO begins with initializing a D-dimensional swarm of particles. Each particle has a position vector  $x_i = [x_{i1}, x_{i2}, \dots, x_{in}] (i = 1, 2, \dots, D)$ , a velocity vector  $v_i = [v_{i1}, v_{i2}, \dots, v_{in}] (i = 1, 2, \dots, D)$ , and a personal best position  $p_i = [p_{i1}, p_{i2}, \dots, p_{in}] (i = 1, 2, \dots, D)$  which is judged by optimization target called adaptive function so far. At the iteration  $t + 1$ , each particle accelerates in the direction of its own personal best position  $p_i$  and the direction of the global best position  $p_g$ . The velocity can be given:

$$v_{ij}(t+1) = \omega v_{ij}(t) + c_1 r_{1j}(t)(p_{ij}(t) - x_{ij}(t)) + c_2 r_{2j}(t)(p_{gj}(t) - x_{ij}(t)) \quad (11)$$

Where  $w$  is the inertia weight typically that is usually set to 0.5,  $c_1$  and  $c_2$  are acceleration constants which are usually set to 1.5, and  $r_{1j}$  and  $r_{2j}$  are uniformly distributed random numbers range from 0 to 1. Equation (12) is given to obtain the next position. Updating its individual best position  $p_i$  and the global best position  $p_g$  on the basis of the new position.

$$x_{ij}(t+1) = x_{ij}(t) + v_{ij}(t+1) \quad (12)$$

Through the above analysis, the process of optimal-capacity current-limiting control method is shown in Fig 2. Current-limiting proportion of each harmonic will be identified by the global best position  $p_g$ .

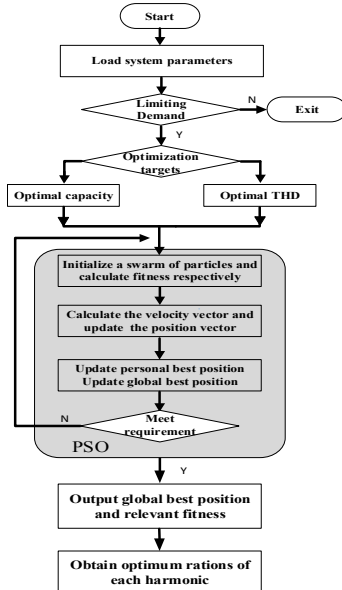


Figure 2. Process of optimal current-limiting control method.

Remarkably, optimal amplitude-limiting strategy exist two respects: 1) Optimal-capacity control which means maximize output capacity of SAPF, 2) Optimal-THD control which means minimize the harmonic distortion rate of grid-side current.

#### B. Current-control strategy

High performance harmonic current controller has an important effect on compensation precision and reliability of SAPF. The traditional the single PI current loop and selective harmonic detection under multiple rotating reference frame is widely used for its easier implementation. However, steady-state error needs to be eliminated to improve the compensation precision according to the bode diagram [16]. This paper adopts an improved control method based on amplitude and phase correction as shown in Fig. 3.

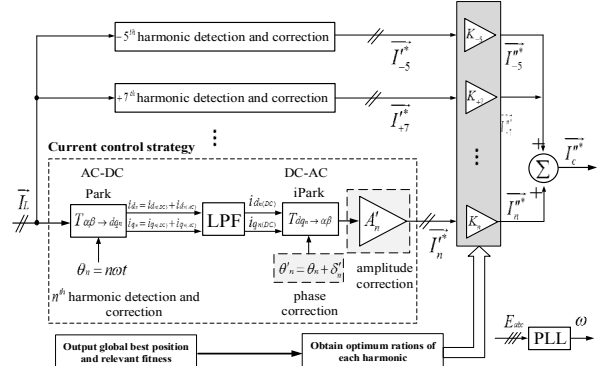


Figure 3. Block diagram of control strategy of improved current-limiting method.

The practical harmonic reference current amplitude and phase correction is

$$\bar{I}_n^* = \bar{I}_n^* K_n e^{j\delta_n'} = \bar{I}_n^* A_n' K_n e^{j\delta_n'} = \bar{I}_n^* K_n e^{j-\delta_n} / A_n \quad (13)$$

In equation (13),  $k_n$  represents current-limiting coefficient which is determined by the global best position,  $A_n'$  represents amplitude correction coefficient, and there is  $A_n' = 1/A_n$ ,  $A_n$  represents amplitude gain,  $\delta_n' = -\delta_n$ , and  $\delta_n$  is phase deviation. When the capacity of SAPF is less than the harmonic capacity, the current-limiting function will be enabled.

### IV. SIMULATION AND EXPERIMENTAL RESULTS

#### A. Simulation results

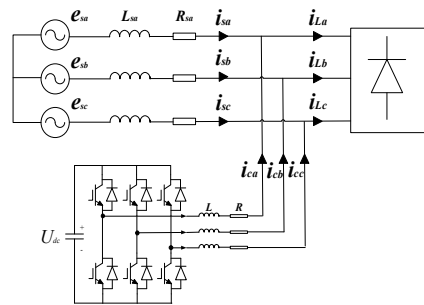


Figure 4. Main circuit topology of SAPF.

Three-phase three-wire SAPF is built for simulation, and main circuit topology is shown in Fig. 4, where,  $U_{dc}$  is the dc-link voltage,  $R$  and  $L$  are the equivalent resistance and filter inductance.  $i_{cx}$ ,  $i_{sx}$  and  $i_{Lx}$  are compensation currents, grid-side current and load current, respectively, where  $x=a, b$  and  $c$ . In addition, the major simulation parameters is shown in Table. I.

TABLE I. SYSTEM PARAMETERS

Parameter	Symbol	Value	Unit
Grid line voltage	$es$	380	V
Grid frequency	$f$	50	Hz
Dc-link voltage	$U_{dc}$	800	V
Dc-link capacitor	$C$	3000	$\mu\text{F}$
Grid-connected inductance	$L$	0.5	mH
Parasitic resistance	$R$	2	m $\Omega$
Sampling frequency	$f_s$	20	kHz
Switching frequency	$f_c$	10	kHz

### 1) Traditional current-limiting control

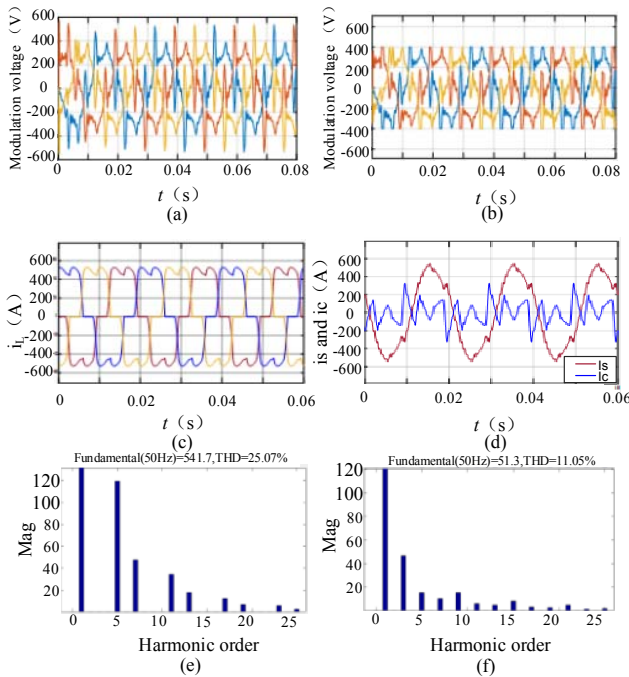


Figure 5. Simulation results of traditional current-limiting strategy.

(a): Modulation voltage without current limitation, (c)(e): Load current and spectrum analysis, (b): Modulation voltage with traditional current limitation, (d)(f): Grid-side current  $I_s$ , output compensation current  $I_c$  and spectrum analysis of  $I_s$ .

As shown in Fig. 5, when the value of modulation voltage exceeds  $U_{dc}/2(400\text{V})$ , the traditional current-limiting control is carried out and the modulation voltage is truncated

and kept in 400V. However, extra undesired harmonic currents will be introduced, and the performance of SAPF is poor due to a low utilization rate.

### 2) Optimal current-limiting control using PSO

The process of searching for the optimum limiting ratios of each harmonic can be seen from Fig. 6(a) and (e). Both in optimum-capacity control and optimum-THD control, the modulation voltage can be limited within  $U_{dc}/2$  effectively. In addition, there is no extra undesired harmonic currents introduced into grid, and the THD of grid-side current are only 5.04% and 4.22% respectively, which verify the effectiveness of the proposed strategy.

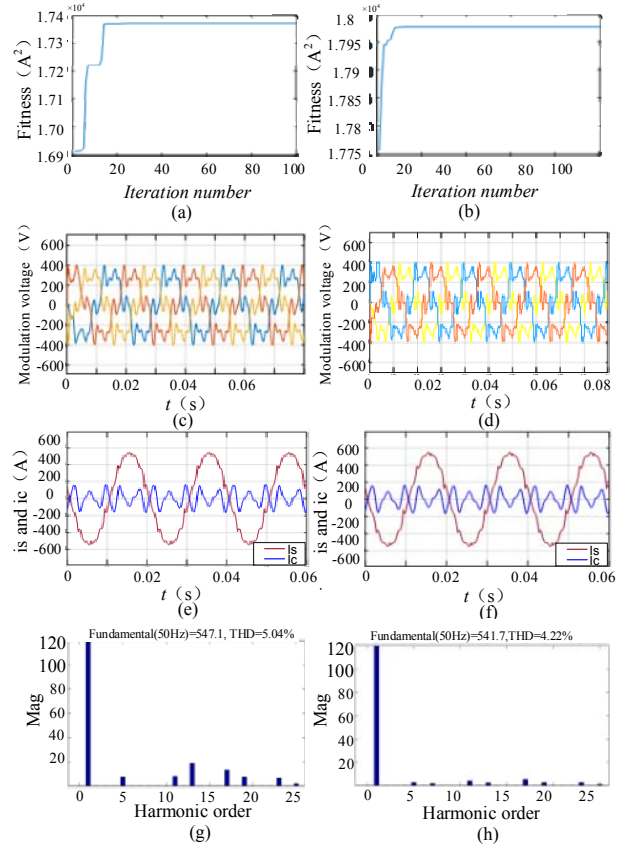


Figure 6. Simulation results of the proposed current-limiting strategy. (a)(c)(e)(g): Simulation waves with the optimum-capacity control strategy, (b)(d)(f)(h): Simulation waves under the optimum-THD control strategy.

### B. Experimental results



Figure 7 Experimental platform.

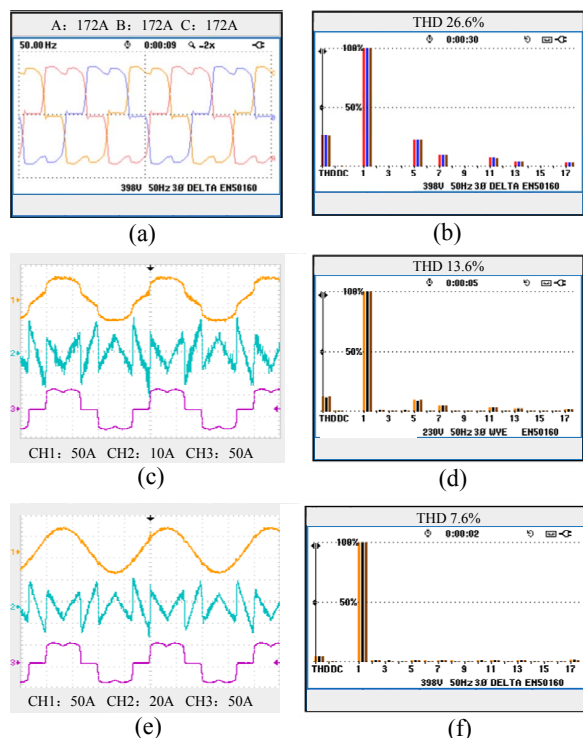


Figure 8: Experimental results.

(a)(b): Load current, (c)(d):Waveform of A phase with the traditional current-limiting strategy, (e)(f): Waveform of A phase with the proposed current-limiting strategy.

The same conclusion can be obtained from the experimental results as shown in Fig. 8. Analyzing grid-side current and its frequency spectrum in Fig. 8(d) and (f), it can be seen obviously that, the grid-side current include much more extra undesired harmonic currents under the traditional current-limiting control. In addition, the utilization rate of SAPF is improved under the optimal current-limiting strategy using PSO, which verified the effectiveness of the proposed current-limiting strategy.

## V. CONCLUSION

An improved current-limiting strategy based on PSO is proposed to optimize the utilization rate of SAPF or the THD of grid-side current. This strategy takes advantages of the two traditional methods: equal-proportion current-limiting control and truncated current-limiting control. Simulation and experiment results prove: the proposed current-limiting scheme can reduce the THD of grid-side current and improve the utilization rate of SAPF effectively, and no extra undesired harmonic will be injected into the power system. Future work will focus on further experiment validation for the effectiveness of the proposed method, especially dynamic performance.

## ACKNOWLEDGMENT

The authors would like to thank the sponsorship of the National Natural Science foundation of China (51607037),

Innovation foundation for Combination of Industry and Scientific Research of Jiangsu Province (BY2016076-09).

## REFERENCES

- [1] Sheng Xu, "An Improved Current-limiting Control Strategy for Shunt Active Power Filter," in IEEE 8th International Power Electronics and Motion Control Conference, 2016, pp. 1306-1311.
- [2] S. J. Chiang and J. M. Chang, "Design and implementation of the parallelable active power filter," in Annual IEEE Power Electronics Specialists Conference, 1999, pp. 406-411.
- [3] P. Mattavelli and F. P. Marafao, "Repetitive-based control for selective harmonic compensation in active power filter," IEEE Transactions on Industrial Electronics, vol. 51, no. 5, pp. 1018-1024, Oct. 2004.
- [4] Y. Tang, P. C. Loh, P. Wang, F. H. Choo, F. Gao, and F. Blaabjerg, "Generalized design of high performance shunt active power filter with output LCL filter," IEEE Transactions on Industrial Electronics, vol. 59, no. 3, pp. 1443-1452, Mar. 2012.
- [5] L. Asiminoaei, C. Lascu, F. Blaabjerg and I. Boldea, "Performance Improvement of Shunt Active Power Filter With Dual Parallel Topology," IEEE Transactions on Industrial Electronics, vol. 22, no. 1, pp. 247-259, Jan. 2007.
- [6] S. K. Khadem, M. Basu and M. F. Conlon, "A review of parallel operation of active power filters in the distributed generation system," in European Conference on Power Electronics and Applications, 2011, pp. 1-10.
- [7] S. J. Chiang and J. M. Chang, "Parallel operation of shunt active power filters with capacity limitation control," IEEE Transactions on Aerospace and Electronic Systems, vol. 37, no. 4, pp. 1312-1320, Oct. 2001.
- [8] J. C. Alfonso-Gil, E. Pérez, C. Ariño and H. Beltran, "Optimization Algorithm for Selective Compensation in a Shunt Active Power Filter," IEEE Transactions on Industrial Electronics, vol. 62, no. 6, pp. 3351-3361, Jun. 2015.
- [9] L. Asiminoaei, E. Aeloiza, P. N. Enjeti, and F. Blaabjerg, "Shunt Active-Power-Filter Topology Based on Parallel Interleaved Inverters," IEEE Transactions on Industrial Electronics, vol. 55, no. 3, pp. 1175-1189, Mar. 2008.
- [10] Liang Xu, Liu Wenhua, Zhu Qingxiang, and Sabri Çamur, "New Development of Protection System of STATCOM," Automation of Electric Power, vol. 24, no. 23, pp. 29-31, Dec. 2000.
- [11] Shang Shaofeng, Zhu Dongbai, and Liu Ji, "Simulation of active power filter in short-circuit faults and its over-current protection," Journal of Harbin University of Science and Technology, vol. 10, no. 1, pp. 58-62, Feb. 2005.
- [12] Mahdi Salimi, Jafar Soltani, and Adel Zakipour, "Experimental design of the adaptive backstepping control technique for single-phase shunt active power filter," IET Power Electronics, vol. 10, no. 8, pp. 1175-1189, Jul. 2017.
- [13] Korhan Karaarslan, Birol Arifoğlu, Ersoy Beşer, and Sabri Çamur, "Single phase series active power filter based on 15-level cascaded inverter topology," in International Conference on Electrical and Electronic Engineering, 2017, pp. 37-42.
- [14] Yang Zhenyu, Zhao Jianfeng, Tang Guoqing, "Research on current limiting compensation scheme of shunt APF," Electric Power Automation Equipment, vol. 26, no. 3, pp. 21-25, Mar. 2007.
- [15] R. Pregitzer, J. G. Pinto, L. F. C. Monteiro and J. L. Afonso, "Shunt active power filter with dynamic output current limitation," in IEEE International Symposium on Industrial Electronics, 2007, pp. 1021-1026.
- [16] Cao Wu, Liu Kangli, Zhaojianfeng, "The analysis of the conditions in which APF need output-limitation and its implementation scheme," Transactions of China Electrotechnical Society, vol. 30, no. 14, pp. 405-411, Jul. 2015.